Intracellular Mg^{2+} and Magnesium Depletion in Isolated Renal Thick Ascending Limb Cells

Long-Jun Dai and Gary A. Quamme
Department of Medicine, University of British Columbia, University Hospital—UBC Site, Vancouver, British Columbia V6T 1W5, Canada

Abstract

Magnesium reabsorption and regulation within the kidney occur principally within the cortical thick ascending limb (cTAL) cells of the loop of Henle. Fluorometry with the dye, mag-fura-2, was used to characterize intracellular Mg^{2+} concentration ($[Mg^{2+}]_i$) in single cTAL cells. Primary cell cultures were prepared from porcine kidneys using a double antibody technique (goat anti-human Tamm-Horsfall and rabbit anti-goat IgG antibodies). Basal $[Mg^{2+}]_i$ was 0.52±0.02 mM, which was ~ 2% of the total cellular Mg. Cells cultured (16 h) in high magnesium media (5 mM) maintained basal $[Mg^{2+}]_i$, 0.48±0.02, in the normal range. However, cells cultured in nominally magnesium-free media possessed $[Mg^{2+}]_i$, 0.27±0.01 mM, which was associated with a significant increase in net Mg transport, (control, 0.19±0.03 and low Mg, 0.35±0.01 nmol · mg^{-1} protein · min^{-1}) as assessed by ^{28}Mg uptake. Mg^{2+}-depleted cells were subsequently placed in high Mg solution (5 mM) and the Mg^{2+} refill rate was assessed by fluorescence. $[Mg^{2+}]_i$ returned to normal basal levels, 0.53±0.03 mM, with a refill rate of 257±37 nM/s. Mg^{2+} entry was not changed by 5.0 mM Ca^{2+} or 2 mM Sr^{2+}, Cd^{2+}, Co^{2+}, nor Ba^{2+} but was inhibited by $Mn^{2+} \simeq La^{3+} \simeq Gd^{3+} \simeq Ni^{2+} \simeq Zn^{2+} \simeq Be^{2+}$ at 2 mM. Intracellular Ca^{2+} and ^{45}Ca uptake was not altered by Mg depletion or Mg^{2+} refill, indicating that the entry is relatively specific to Mg^{2+}. Mg^{2+} uptake was inhibited by nifedipine (117±20 nM/s), verapamil (165±34 nM/s), and diltiazem (194±19 nM/s) but enhanced by the dihydropyridine analogue, Bay K 8644 (366±71 nM/s). These antagonists and agonists were reversible with removal and $[Mg^{2+}]_i$ subsequently returned to normal basal levels. Mg^{2+} entry rate was concentration and voltage dependent and maximally stimulated after 4 h in magnesium-free media. Cellular magnesium depletion results in increases in a Mg^{2+} refill rate which is dependent, in part, on de novo protein synthesis. These data provide evidence for novel Mg^{2+} entry pathways in cTAL cells which are specific for Mg^{2+} and highly regulated. These entry pathways are likely involved with renal Mg^{2+} homeostasis. (*J. Clin. Invest.* 1991. 88:1255–1264.) Key words: cortical thick ascending limb • epithelial cells • fluorescence • kidney • Mg^{2+} entry • primary culture

Address reprint requests to Dr. Gary Quamme, Department of Medicine, University Hospital—UBC Site, 2211 Wesbrook Mall, Vancouver, BC V6T 1W5, Canada.

Received for publication 26 December 1990 and in revised form 3 May 1991.

J. Clin. Invest.

0021-9738/91/10/1255/10 $2.00
Volume 88, October 1991, 1255–1264

Introduction

Homeostasis of total body magnesium occurs principally within the kidney by epithelial cells of the cortical segment of the thick ascending limb (cTAL)[1] of Henle's loop (1–3). Shareghi and Agus (4), using in vitro perfused tubules, provided evidence for passive magnesium transport probably moving through the paracellular pathway. These early observations were supported by the findings of de Rouffignac and colleagues (1, 5). However, the later investigators also showed that magnesium transport may be altered in the absence of voltage and resistance changes and NaCl absorption, suggesting that magnesium transport may be active in nature (5).

Although we have considerable understanding of transepithelial magnesium movement and some of the factors that control transport, little is known about the intracellular regulation of magnesium (1–5). This, has been due in part to the lack of an adequate radiotracer of magnesium or other suitable quantitative methods (2, 6). More important was the deficiency of an adequate means of assessing free Mg^{2+} activity. The recent development of fluorescent dyes for Mg^{2+} should allow a better understanding of cellular free Mg^{2+} movements (7). It is the free Mg^{2+} concentration ($[Mg^{2+}]_i$) that is thought to be important in determining plasma membrane transport and entry into biochemical processes rather than total magnesium, much of which is bound to intracellular ligands (6). The use of mag-fura-2 to assess $[Mg^{2+}]_i$ may not clarify an understanding of paracellular vs. intracellular magnesium absorption but it could contribute to our knowledge of intracellular Mg^{2+} control.

The purpose of the present study was to characterize some of the controls of intracellular $[Mg^{2+}]$ in isolated cTAL epithelial cells. A cell model was developed to evaluate the influx pathway. Isolated cTAL cells were initially depleted of magnesium and then subsequently placed in buffer containing high magnesium concentrations; the refill of $[Mg^{2+}]_i$ was monitored as a function of time to assess the influx pathway. The results indicate that this influx pathway is specific to Mg^{2+}, is inhibited by a number of channel blockers, and is highly regulated. These findings may be relevant to magnesium absorption in the thick ascending limb of Henle's loop.

Methods

Isolation of cTAL cells. cTAL cells were isolated by a double-antibody technique according to the methods of Smith and co-workers (8, 9). Briefly, tissue from the innermost fifth of the cortex (beginning 1–2 cm above the outer red medulla and extending toward the cortex) was obtained from porcine kidneys. The tissue was gently minced and

1. *Abbreviation used in this paper:* cTAL, cortical thick ascending limb.

added to 0.1% collagenase in Hepes-buffered Krebs solution (in mM): KCl 5, NaCl 145, Na_2HPO_4 1, $CaCl_2$ 1, $MgCl_2$ 0.5, glucose 5, Hepes 10, pH 7.4. This tissue was diluted to 40 ml of buffer containing 0.1% collagenase and incubated for 5 min in a shaker bath at 37°C. Control of this step is critical because overtreatment with enzymes decreases viability of the cTAL cells. After the tissue was dispersed with collagenase, the mixture was centrifuged at 700 rpm for 2 min and the supernatant was removed. The tissue pellet was resuspended and centrifuged through 10 ml of 10% BSA to remove subcellular debris (8). The pellet (350–400 mg of protein) containing tubular fragments and single cells was resuspended in an admixture of DME and Ham's F12 (1:1) media. Goat anti-human uromucoid serum (50 mg of protein/ml) was added (100 μl/10 ml) to the cellular mixture and incubated for 30 min on ice. The cells were washed twice with PBS (pH 7.4) by gentle centrifugation. Cell suspensions (4 ml) were added sequentially to plastic petri plates (80 mm, Corning Glass, Inc., Corning, NY) previously coated with 80 μg of rabbit anti-goat IgG as detailed by Allen et al. (9). The cells were rocked on the antibody-coated dishes for 3–5 min at 21°C. Each dish was then washed six times with 5-ml aliquots of PBS. The attached cells were subsequently dislodged by a sharp tap on the plate and collected by gentle centrifugation. The pelleted cells were dispersed with DME-Ham's F12 culture media and grown on the appropriate support in 95%/5%, air/CO_2. Our experience with cell isolation from porcine kidneys were similar to those reported for the rabbit by Allen and coworkers (9, 10). Cultured cTAL cells were used between 7 and 14 d after the primary isolation.

Characteristics of isolated cTAL cells. Hormone-induced cAMP formation was determined after 10 min of incubation with agonist or vehicle and 10^{-3} M isobutylmethyl xanthine (IBMX) in cells cultured for 4–6 d on plastic supports. cAMP concentrations were assayed by radioimmunoassay with kit no. 6021 from Sigma Chemical Co., St. Louis, MO. Protein was determined by the Lowry method after solubilization of cells with 1% SDS.

cTAL cells demonstrate bumetanide-sensitive $Na^+/K^+/Cl^-$ cotransport; accordingly, K^+ influx was assessed to characterize cTAL function. Bumetanide-sensitive ^{86}Rb uptake was assayed in confluent cTAL cells cultured on plastic supports or grown on collagen-coated filters (Millipore Corp., Bedford, MA). ^{86}Rb is a congener of K^+ (11). Cell monolayers were washed three times with Krebs-Ringer buffer without potassium and then incubated in Krebs-Ringer transport solution, containing 1 mM KCl, 0.2 mM ouabain, and 5.0 mM $BaCl_2$ with and without 0.1 mM bumetamide. After 5 min, the uptake was stopped with ice-cold buffer, the cells were extracted with 0.5% Triton X-100 and ^{86}Rb uptake was determined by liquid-scintillation spectroscopy (11). Uptake values were expressed per mg cellular protein as determined by the procedure of Lowry.

Determination of cytosolic free Mg^{2+} and Ca^{2+}. Isolated cTAL cells were loaded with 10 μM fura-2/AM or 5 μM mag-fura-2/AM accordingly to previously described techniques (12). The fluorescent dye, dissolved in dimethylsulfoxide (DMSO), was added directly to the medium with the aid of Pluronic F-127 (0.125%; Molecular Probes, Inc., Eugene, OR) and incubated for 30 min at 23°C. The final concentration of DMSO in the incubation medium did not exceed 0.2%. Loaded cells were washed twice with a buffered salt solution (in mM): NaCl 145, KCl 4.0, $CaCl_2$ 1.0, Na_2HPO_4 0.8, KH_2PO_4 0.2, glucose 18, and Hepes-Tris 20, pH 7.4. The cells were incubated a further 20 min to ensure complete de-esterification and finally washed once with fresh buffer solution. $MgCl_2$ was added from stock solutions to yield various concentrations as given in legend to figures. Cover glasses, with cells loaded with fura-2, were mounted in a chamber containing 500 μl of buffer placed on the mechanical stage of an inverted microscope (Diaphot, Nikon Inc., Melville, NY). The fluorescence signal was monitored at 510 nm with excitation wavelengths alternating between 340 and 385 nm for mag-fura-2 and 335 and 385 for fura-2 using a spectrofluorometer (Deltascan, Photon Technologies, Inc., Santa Clara, CA). The $[Ca^{2+}]_i$ was calculated as described by Grynkiewicz et al. (13) with a K_D of 224 nM for the fura-2 · Ca^{2+} complex after correction for fluorescence from extracellular fura-2 and autofluorescence according to previously described methods. For the calculation of $[Ca^{2+}]_i$ we defined the maximum (R_{max}) and minimum (R_{min}) fluorescence ratios as the ratios of the fluorescence at 335 and 385 nm measured in cells incubated in the above solution containing 2 mM $CaCl_2$ and 10 μM digitonin and those in cells incubated in the above solution containing no Ca^{2+}, 10 μM digitonin, and 20 mM EGTA (pH 8), respectively. In separate preparations, $[Mg^{2+}]_i$ was determined with mag-fura-2. For measurement of $[Mg^{2+}]_i$, the procedure was similar to Ca^{2+} with the following exceptions. cTAL cells, on glass coverslips, were loaded with mag-fura-2/AM (5 μM) in the above media for 30 min at 23°C. After loading, the cells were washed twice as above, and kept at room temperature until cytosolic Mg^{2+} was measured. Free Mg^{2+} values were monitored through the fluorescent signals of mag-fura-2 at excitation wavelengths of 340 and 385 nm. Cells were permeabilized with 10 μM digitonin in the presence of 50 mM magnesium to obtain maximal fluorescence (R_{max}) of the mag-fura-2 · Mg^{2+} complex. This was washed once, followed by the addition of 50 mM EDTA and 20 mM Tris buffer at pH 8.5 to determine R_{min} values. Free Mg^{2+} was determined as previously described (12) using a K_D of 1.45 mM for the mag-fura-2 · Mg^{2+} complex. In all experiments involving Mg^{2+} analyzes single traces are shown, but similar results were obtained in at least three separate experiments from independent cell preparations.

Representative fluorescent tracings are shown. All results are expressed as means±SE where indicated. The change in $[Mg^{2+}]_i$ with time was determined where appropriate by linear regression analysis of the tracing over the time interval of interest. Significance was determined by one-way analysis of variance. A probability of $P < 0.05$ was taken to be statistically significant.

Total magnesium was determined in cTAL cells by atomic absorption spectrophotometry according to the methods of Elin and Johnson (14). Confluent cell monolayers were dissolved for 1 h in 12% perchloric acid before magnesium determination. Total magnesium content is expressed as micrograms per milligram protein (14).

^{28}Mg and ^{45}Ca uptake measurements. ^{28}Mg and ^{45}Ca uptake was performed by methods similar to those previously described (15). Incubations were routinely performed at 5 min with transport solution containing (in mM): NaCl 137, KCl 5.4, Na_2HPO_4 1.0, Hepes-Tris 14, pH 7.4, and $^{45}CaCl_2$ 0.1, or $^{28}MgCl_2$ 0.1. Incubations were terminated by rapid aspiration of the transport solution and addition of ice-cold solution and the cells were solubilized in 0.5% Triton X-100 for 1 h. ^{28}Mg or ^{45}Ca uptake by the cells was measured by liquid scintillation on 150 μl of extract solution. ^{28}Mg and ^{45}Ca uptake was normalized according to total protein content.

Materials. Dulbecco's modified Eagles' medium (DME) and Ham's F12 (1:1) medium containing D-glucose (5.0 g/L), L-glutamine (5 mM), 10% FCS was from Gibco Laboratories, Grand Island, NY. Goat anti-human uromucoid (Tamm-Horsfall glycoprotein) serum was purchased from Organon Teknika, Rockville, MD, and affinity-purified rabbit anti-goat IgG was from Sigma Chemical Co. Parathyroid hormone, arginine vasopressin, calcitonin, and glucagon were from Sigma Chemical Co. Collagenase, type V-S, was from Sigma Chemical Co., ^{86}Rb and ^{131}I-cAMP assay kit were obtained from Amersham Corp., Arlington Heights, IL, and ^{28}Mg was from Martin-Maretta, Oak Ridge National Laboratories, Oak Ridge, TN. Fura-2 and mag-fura-2 were obtained from Molecular Probes, Inc. All other chemicals were purchased from Sigma Chemical Co. or Fisher Scientific Co., Pittsburgh, PA.

Results

Characteristics of primary cultured cTAL cells. The isolated cTAL cells grown to confluence for 5–6 d had a morphological appearance of epithelial cells. They had a cuboidal ultrastructure when grown on filters and they developed small domes, five to six cells in diameter, when cultured on solid supports for 10–14 d (10).

Isolated cTAL cells were responsive to various hormones known to release cAMP in the thick ascending limb (1). Basal cAMP concentrations were 25.9±1.0 pmol · mg^{-1} protein · 10 min^{-1}. Parathyroid hormone (10^{-7} M), antidiuretic hormone

(10^{-7} M), and calcitonin (10^{-7} M) stimulated cAMP release by 1.3±0.2-, 3.2±0.1-, and 1.8±0.1-fold (n = 4), respectively, in cells cultured for 5–6 d on plastic supports. Glucagon (10^{-6} M) failed to stimulated cAMP formation in cultured cTAL cells, which is in concert with the observations of Allen et al. (9). However, when cAMP production was measured on the cell suspension prepared from the renal tissue, glucagon stimulated cAMP release by 1.52-fold (n = 2). Accordingly, the glucagon receptor does not appear to be exposed in cTAL cells cultured on supports although it is present at the time of cell isolation (8). The presence of receptors for parathyroid hormone, calcitonin, antidiuretic hormone, and glucagon indicates that these cells originated from the cTAL (1).

The cTAL cells demonstrated Na/K/Cl cotransport as indicated by bumetanide-sensitive ^{86}Rb uptake; amounting to 40% of control uptake which was 0.47±13 nmol·mg^{-1} protein·min^{-1} (n = 3). The above characteristics indicate that the cultured cells have retained many of the assayed functions typical of thick ascending limb cells within the intact kidney.

Basal Mg^{2+} levels. The mean basal concentrations of intracellular Mg^{2+} is 0.52±0.02 mM, n = 30 (Fig. 1). The distribution of cellular concentrations around the mean value followed a normal fashion (Fig. 2). The mean $[Mg^{2+}]_i$ for cTAL cells was significantly greater than MDCK cells, 0.49±0.03 mM, n = 7 (15) or isolated cardiomyocytes, 0.46±0.01 mM, n = 56 (12). Since intracellular Mg^{2+} is in the order of 0.5 mM, only 1–2% of the total cell magnesium is in the free form.

In order to assess changes in $[Mg^{2+}]_i$ in response to extracellular magnesium, cTAL cells were first cultured for 16–20 h in media containing high magnesium concentrations (5.0 mM). $[Mg^{2+}]_i$ was 0.48±0.02 mM, n = 5, and total magnesium was 1.43±0.21 μg/mg protein. Total magnesium concentration was not altered with elevated extracellular magnesium concentrations and $[Mg^{2+}]_i$ was actually lower than cells cultured in normal media containing 0.6 mM magnesium. On the other hand, culturing the cells for 16–20 h in the absence of magnesium resulted in Mg^{2+} depletion, 0.27±0.01 mM, n = 78; however, there were no detectable changes in total magnesium, 1.38±0.19 μg/mg protein, n = 4.

Identification of Mg^{2+} influx pathway. We developed the following model to establish the presence of an influx pathway in isolated cTAL cells (12, 15). Confluent cTAL monolayers were cultured in magnesium-free medium for 16–20 h. These cells possessed a significantly lower $[Mg^{2+}]_i$ as indicated in Fig. 1, which was a very reproducible 0.27±0.01 mM, n = 78. When the depleted cTAL cells were placed in a bathing solution containing 5 mM $MgCl_2$, intracellular $[Mg^{2+}]$ concentration increased in a linear fashion with time and abruptly leveled at a $[Mg^{2+}]_i$ (0.53±0.03 mM, n = 24) which was similar to normal cells (Fig. 1). The rate of refill, $d([Mg^{2+}]_i)/dt$, measured as the change in $[Mg^{2+}]_i$ with time, was 258±37 nM·s^{-1}, n = 11. There was no change in intracellular $[Ca^{2+}]$ after the addition of $MgCl_2$ to the bathing medium either in normal or magnesium-depleted cTAL cells. The following studies will indicate that this influx pathway is distinctive and regulated by intracellular Mg^{2+} concentrations.

Fig. 3 illustrates the effect of cellular magnesium depletion on net ^{28}Mg uptake into cells. Net ^{28}Mg uptake was significantly greater in isolated cells grown in magnesium-deficient media compared with those cells cultured in normal media containing 0.6 mM magnesium, confirming the notion that these epithelial cells can intrinsically adapt their transport rates accordingly to the availability of magnesium. We and others (2, 16) have shown that the intact kidney increases magnesium reabsorption in response to magnesium depletion such as that which occurs after consumption of magnesium-deficient diets. Net ^{45}Ca uptake rates were similar in confluent cTAL cells cultured in normal media or magnesium-deficient media (0.70±0.07 vs. 0.61±0.07 nmol·mg^{-1} protein·min^{-1}, respectively). Our interpretation of these findings is that the adaptative response to low magnesium media is specific to magnesium which is consistent with the observations within the intact kidney where magnesium transport rates may be altered without associated changes in calcium transport (16).

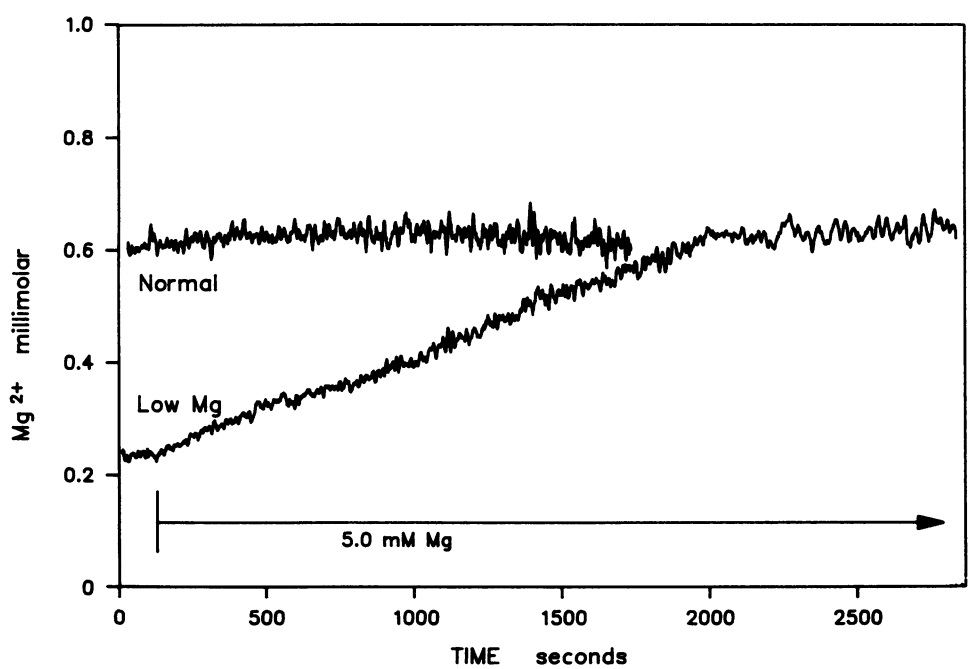

Figure 1. Intracellular Mg^{2+} concentration of single confluent cTAL cells. $[Mg^{2+}]_i$ was determined with mag-fura-2. Cells were cultured in normal media ([Mg], 0.6 mM and [Ca], 1.0 mM) or low Mg media (< 0.01 and 1.0 mM, respectively). The basal $[Mg^{2+}]_i$ was determined and the cells subsequently placed in buffer solution containing high magnesium concentration (5.0 mM). The Mg^{2+} refill rate was calculated as a change in Mg^{2+} concentration with time ($d([Mg^{2+}]_i/dt)$ by linear regression analysis. Fluorescence was measured at 1 data point/s with 25 signal averaging and smoothed according to methods previously reported (12).

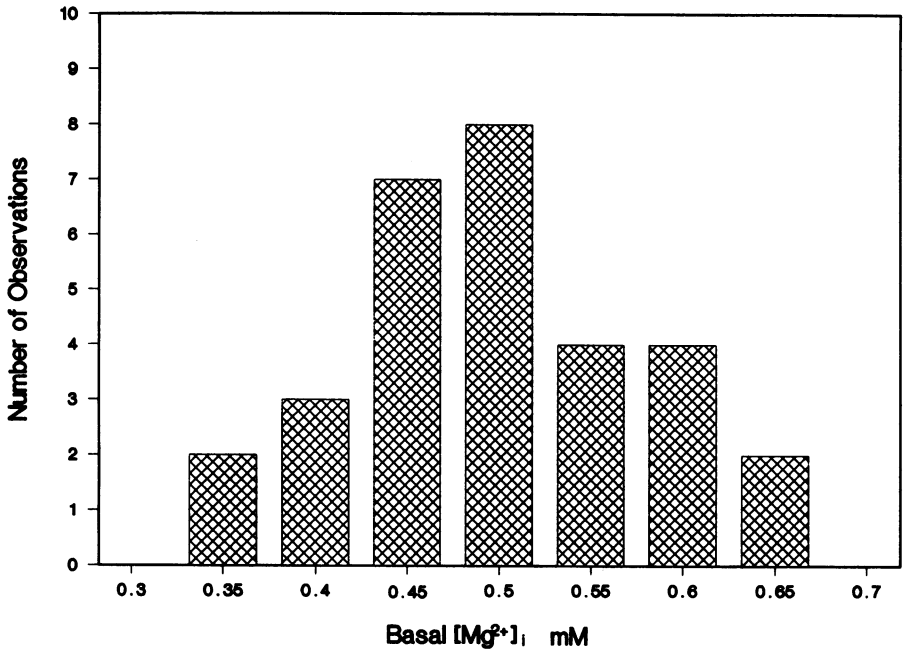

Figure 2. Distribution of normal $[Mg^{2+}]_i$ in single confluent cTAL cells. $[Mg^{2+}]_i$ was determined as given in the legend to Fig. 1. Intracellular (Mg^{2+}) follows a normal distribution with a mean value of 0.52±0.02 mM.

Specificity of the Mg^{2+} influx pathway. A number of inorganic cations were used to determine the specificity of the Mg^{2+} influx pathway. The effect of 5 mM external Ca^{2+} was tested by adding it with the 5.0 mM $MgCl_2$ refill solution. Calcium had no effect on the intracellular refill rate for Mg^{2+} (Table I), suggesting that the putative Mg^{2+} pathway is distinct from Ca^{2+} entry. This observation is in concert with the in vivo microputncture studies (2) which clearly show that there is no inhibition of magnesium reabsorption with elevation of luminal or apical calcium in the loop of Henle. There were no changes in $[Ca^{2+}]_i$ during these manipulations over the duration of study (data not shown).

Fig. 4 demonstrates the effect of La^{3+} on the Mg^{2+} influx pathway. La^{3+}, 5.0 mM, completely inhibited the change in $[Mg^{2+}]_i$ when added concurrently with $MgCl_2$. Removal of the La^{3+} resulted in an immediate increase in $[Mg^{2+}]_i$ in the presence of external magnesium; the rate of change, 278±35 $nM \cdot s^{-1}$, was similar to control cells and abruptly stopped at or near-normal cellular $[Mg^{2+}]_i$. Similar studies were performed, but with fura-2 to measure $[Ca^{2+}]_i$; $[Ca^{2+}]_i$ was normal in magnesium-depleted cells and La^{3+} had no effect on calcium levels over the time period of study. These studies indicate that the entry of Mg^{2+} is due to the presence of a mediated pathway rather than simple diffusion of Mg^{2+} across the plasma membrane into the cell. Although conductivity measurements have not been determined, this mediated pathway may be a Mg^{2+} channel.

Table I lists the results of a number of other cations on the Mg^{2+} refill rate. Strontium, cadium, cobalt, and barium were without effect on Mg^{2+} entry. Manganese, nickel, zinc, gadolinium, and beryllium inhibited Mg^{2+} entry. The potency sequence approximated: $Mn^{2+} \simeq La^{3+} \simeq Gd^{3+} \simeq Ni^{2+} \simeq Zn^{2+}$ $Be^{2+} \gg Ba^{2+} \simeq Co^{2+} \simeq Cd^{2+} \simeq Sr^{2+} \simeq Ca^{2+}$. Many of these cations alter transmembrane voltage; no attempt was made to correct this sequence for other effects such as changes in voltage. These cations did not have any effect on basal $[Mg^{2+}]_i$ in normal cells cultured in normal magnesium media in the timeframe of study used here (data not shown). In most cases, the inhibition with the inorganic cations was reversible as the refill rate returned to near normal values (Table I). The notable exceptions were Ni^{2+} and Be^{2+} where the refill rates were 182±48 and 109±12 $nM \cdot s^{-1}$, respectively.

Inhibition of Mg^{2+} entry by organic Ca^{2+} channel blockers. Next, we tested a number of organic Ca^{2+} channel blockers for their ability to inhibit Mg^{2+} refill in magnesium-depleted cells (17–19). Nifedipine, a 1,4 dihydropyridine derivative, inhibited the Mg^{2+} influx pathway (Fig. 5). This inhibition was fully reversible after removal of the agent. Bay K 8644, an analogue of nifedipine which increases the open-time of voltage-sensitive

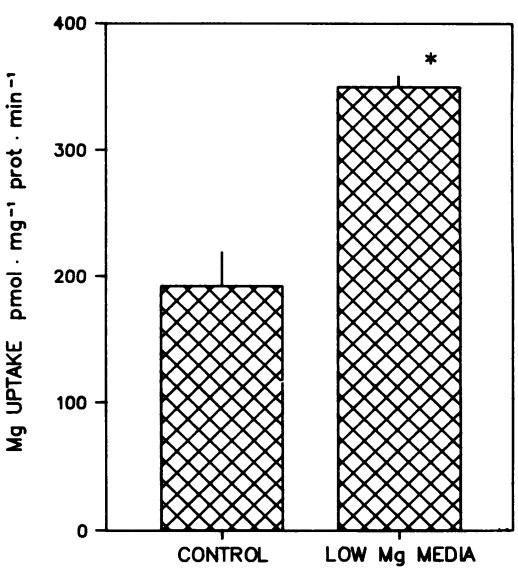

Figure 3. Stimulation of net ^{28}Mg uptake in magnesium-depleted cTAL cells. cTAL cells were grown to confluence (7–14 d) in DME/Ham's F12 containing 0.6 mM magnesium. Monolayers were then cultured in normal (0.6 mM) or low magnesium (< 0.01 mM) media for 16 h before study. Magnesium uptake was determined with 0.1 mM ^{28}Mg over 5 min. Incubations were terminated by rapid aspiration of the transport solution and addition of ice-cold stop solution. Cells were solubilized in 0.5% Triton X-100 and ^{28}Mg was determined on the extraction solution.

Table I. Inhibition of Mg^{2+} Influx with Inorganic Cations

Cation	Concentration	Increment in $[Mg^{2+}]_i$ (presence of cation)	Inhibition	Increment in $[Mg^{2+}]_i$ (following removal of cations)	(n)
	mM	*nM·s⁻¹*	*Percentage of control*	*nM·s⁻¹*	
Control		257±37	100±14		(11)
Mn^{2+}	2.0	40±69*	15±27*	189±71	(4)
La^{3+}	2.0	81±54*	32±21*	246±111	(3)
Gd^{3+}	2.0	80±49*	31±19*	189±71	(2)
Ni^{2+}	2.0	120±23*	47±9*	182±48*	(3)
Zn^{2+}	2.0	160±78*	62±30*	377±90*	(3)
Be^{2+}	2.0	176±13*	68±5*	109±12*	(2)
Ba^{2+}	2.0	232±40	90±16	167±34	(3)
Cd^{2+}	2.0	351±42	136±16	406±157	(3)
Co^{2+}	5.0	248±18	96±7	233±15	(3)
Sr^{2+}	5.0	272±76	106±29	325±51	(3)
Ca^{2+}	5.0	257±74	100±29	204±62	(4)

cTAL were magnesium-depleted, as given in the text, and the increase in $[Mg^{2+}]_i$ assessed in the presence and absence of the various cations according to methods given in Fig. 4. Values are means±SE. * Significance ($P < 0.01$) from control.

Ca^{2+} channels, increased the rate of change of $[Mg^{2+}]_i$ (Fig. 5). Verapamil, a phenylalkylamine, and diltiazem, a benzothiazepine derivative, also inhibited Mg^{2+} refill but to a lesser extent compared to nifedipine (Table II). The apparent potency sequence of these channel blockers is in the order of: nifedipine > verapamil = diltiazem. These findings suggest that Mg^{2+} entry may be through a channel with a close homology to Ca^{2+} channels. Further studies are required to establish this point.

The concentrations of the traditional channel blockers used here are relatively high; but the external magnesium concentration used for refill is also high, 5 mM. We choose this concentration because this value approximates the intraluminal magnesium concentration which is normally found in the ascending limb of Henle's loop (1, 2). To test whether smaller concentrations of blockers may inhibit Mg^{2+} uptake, we performed studies with various concentrations of nitrendipine, another 1,4 dihydropyridine analogue, and external magnesium concentrations of 0.25, 1.0, and 25 mM. A Dixon plot was used to obtain an apparent K_i value of 0.94 μM (Fig. 6). These studies indicate that the effective concentration of blocker required for the inhibition is dependent on the external magnesium concentration used for refill.

Pimozide, a neuroleptic agent, which has also been shown to block Ca^{2+} channels (19, 20), also inhibited Mg^{2+} influx in cTAL cells (Table II). Antagonism by this drug was poorly reversible after removal and extensive washing with pimozide-free buffers.

A number of other selective and semi-selective agents were used to characterize the specificity of Mg^{2+} entry into cTAL cells. Quinidine, a fast Na^+ channel blocker, and tetrodotoxin, an inhibitor of Na^+ channels were tested. These agents also have been reported to inhibit Na^+-Mg^{2+} exchange in red blood cells (21–23) and squid axons (24). Quinidine and tetrodotoxin had no effect on Mg^{2+} refill into magnesium-depleted cells (Table III) suggesting that sodium ions are not directly involved with Mg^{2+}; entry for instance, though a putative Na^+-Mg^{2+} exchanger (21–24). Amiloride, an inhibitor of Na^+ channels, had no effect on Mg^{2+} refill but dichlorobenzamil, a potent inhibitor of Na^+ transport and Na^+-Ca^{2+} exchange (25, 26) had modest effects on refill. The basis for this latter observation is unknown. On balance, these studies would suggest that Na^+-Mg^{2+} is not directly involved with Mg^{2+} entry into cTAL cells.

Concentration dependence of Mg^{2+} refill rate. Fig. 7 illustrates the effect of external magnesium on the refill rate, $d([Mg^{2+}]_i)/dt$, in cells grown in nominally magnesium-free media for 16–20 h. The concentration dependence of the Mg^{2+} flux can be described by Michaelis-Menten kinetics (27, 28). The J_{max} (maximal $d([Mg^{2+}]_i)/dt$) is in the order of 210±18

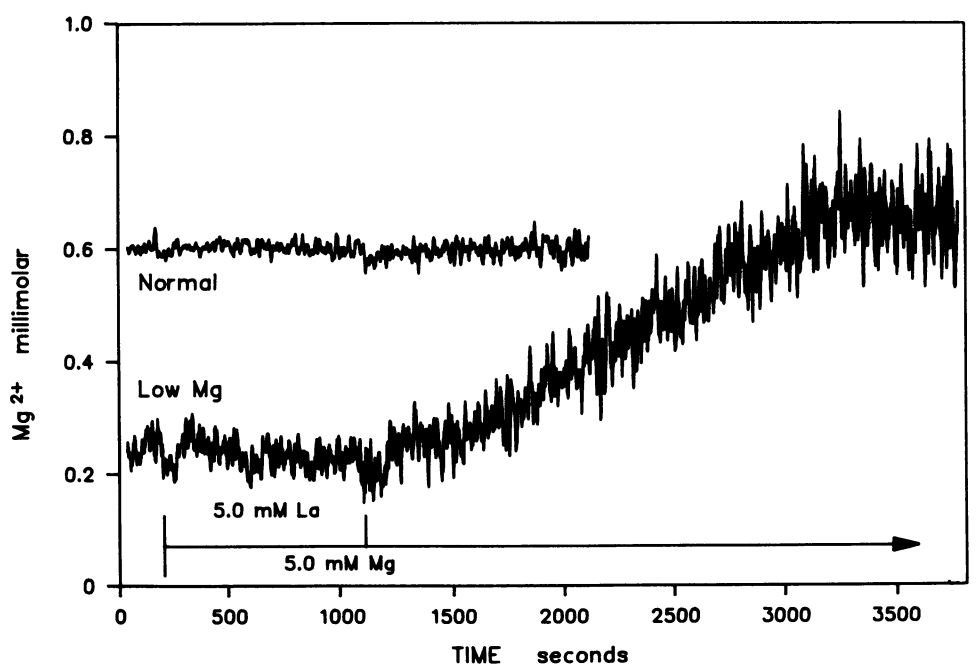

Figure 4. Specificity of Mg^{2+} influx pathway. Intracellular Mg^{2+} concentration was assessed in normal or magnesium-depleted cTAL cells. $LaCl_3$ was added from a stock solution to a final concentration of 5.0 mM with 5.0 mM $MgCl_2$. At the time indicated, $LaCl_3$, was removed by washing three times in buffer solution.

Table II. Effect of Organic Ca^{2+} Channel Blockers and Activators on Mg^{2+} Influx Pathway

Blocker	Concentration	$d([Mg^{2+}]_i)/dt$ (presence of blocker)	Inhibition	$d([Mg^{2+}]_i)/dt$ (removal of blocker)	(n)
	μM	$nM \cdot s^{-1}$	*Percentage of control*	$nM \cdot s^{-1}$	
Control		257±37	100±14		(11)
Nifedipine	42	117±20*	45±8*	243±106	(5)
Bay K 8644	10	366±71*	142±27*	107±9*	(3)
Verapamil	20	165±34*	64±13*	201±22	(3)
Diltiazem	70	194±19*	75±7*	227±36	(3)
Pimozide	100	114±40*	44±15*	56±49*	(4)

Mg^{2+} influx was determined in magnesium-depleted cells as illustrated in Fig. 3. Values are mean±SE. * Significance ($P < 0.01$) from control values.

$nM \cdot s^{-1}$ and the K_m (apparent affinity), the magnesium concentration which results in half-maximal refill rate, is in the order of 0.27±0.12 mM. It is important to note that the final $[Mg^{2+}]_i$ at which the refill rate abruptly leveled off is independent of the external magnesium concentration used in the refill solution supporting the notion that the Mg^{2+} entry pathway is highly regulated in part by the $[Mg^{2+}]_i$. Moreover, as appreciable refill was observed even with 0.05 mM magnesium outside to 0.26 mM inside; the transmembrane electrical gradient likely provides the driving force for Mg^{2+} entry into the epithelial cells.

Effect of transmembrane voltage on Mg^{2+} refill rate. As $d([Mg^{2+}]_i)/dt$ was linear with time from the start of refill to the abrupt termination of refill (Fig. 1), we postulate that the transmembrane voltage may be the basis for movement of Mg^{2+} into the cell. To test this postulate, we determined the rate of refill of cells in which the transmembrane voltage was abolished. cTAL cells were treated with 100 μM ouabain and 2 μM gramicidin D, with and without a transmembrane magnesium chemical gradient. Gramicidin D, a sodium ionophore, was used to ensure complete Na^+ equilibrium across the plasma membrane. The $d([Mg^{2+}]_i)/dt$ was significantly diminished when the transmembrane potential was abolished (Table IV). There was virtually no uptake of Mg^{2+} when there was no transmembrane magnesium concentration gradient. Uptake was not appreciable until the outside-to-inside gradient was 50 to 0.25 mM. Abolishing the voltage decreased the J_{max} to about 103±1 $nM \cdot s^{-1}$ and increased the apparent K_m value to 6.2±3.1 mM (28). Secondly, a bathing solution composed of high K^+, low Na^+ was used which would be expected to depolarize the transmembrane electrical gradient. Mg^{2+} influx was completely inhibited in the presence of high K^+, low Na^+ solutions. These studies support the notion that Mg^{2+} entry into the cell is altered by changes in the transmembrane voltage.

Time dependence for Mg depletion. Intracellular $[Mg^{2+}]_i$ and refill was determined in cTAL cells cultured in low magnesium media for various periods of time. Fig. 8 summarizes these findings. Basal $[Mg^{2+}]_i$ fell within 4 h after placement of the cells in magnesium-free media. Maximal decreases in $[Mg^{2+}]_i$ were attained at ~ 8 h and did not decrease below 0.26 mM even with extended periods of Mg^{2+}-depletion. Refill of Mg^{2+}, $d([Mg^{2+}]_i)/dt$, was determined on these cells depleted for various periods of time. Interestingly, the refill rates were associated with the starting $[Mg^{2+}]_i$ (Fig. 8). This would suggest the Mg^{2+} influx rate is highly dependent on the $[Mg^{2+}]_i$. Furthermore, the channel activity does not increase immediately upon a decrease of $[Mg^{2+}]_i$ but the cell requires a period of time, at least 4 h, to adjust transport rates.

Requirement for protein synthesis. The adaptation in transport rates or channel activity may require de novo synthesis of protein. Accordingly, we used actinomycin D, an inhibitor of transcription (29); cycloheximide, an inhibitor of translation (30); and 3'-deoxyadenosine (cordycepin), an inhibitor of polyadenylation involved in the processing of heterogeneous nuclear RNA (31–34) to determine the role of protein synthesis in the adaptation of $d([Mg^{2+}]_i)/dt$ to magnesium depletion. The

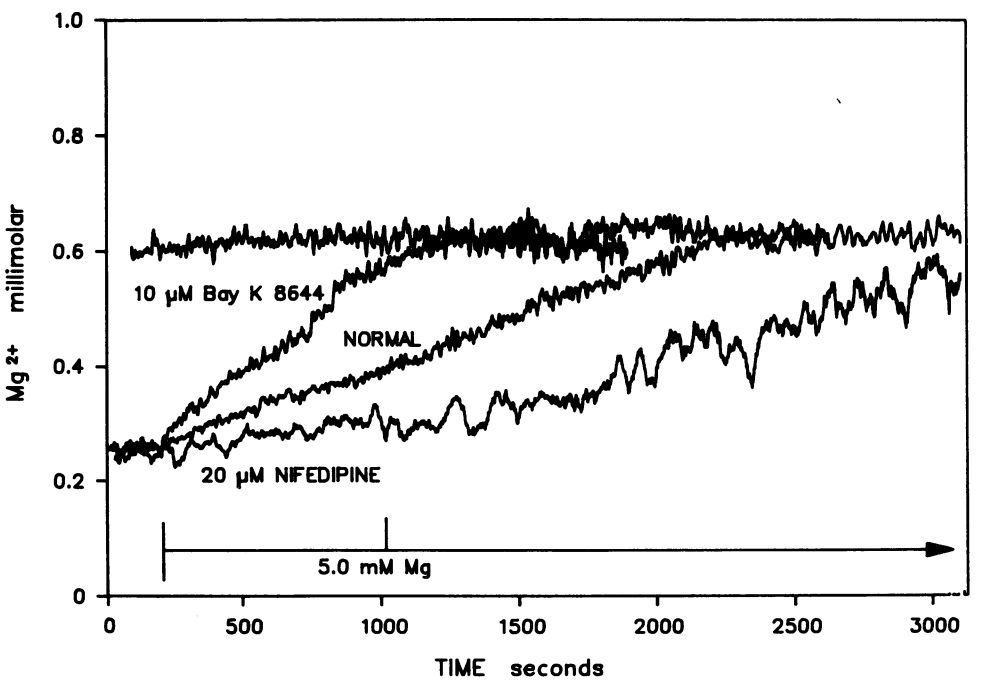

Figure 5. Effect of dihydropyridine antagonists and agonists on Mg^{2+} influx pathway. Refill was assessed by the change in $[Mg^{2+}]_i$ as given in Fig. 1. Nifedipine, 20 μM, and Bay K 8644, 10 μM, were added and removed, as indicated, to the buffer solution.

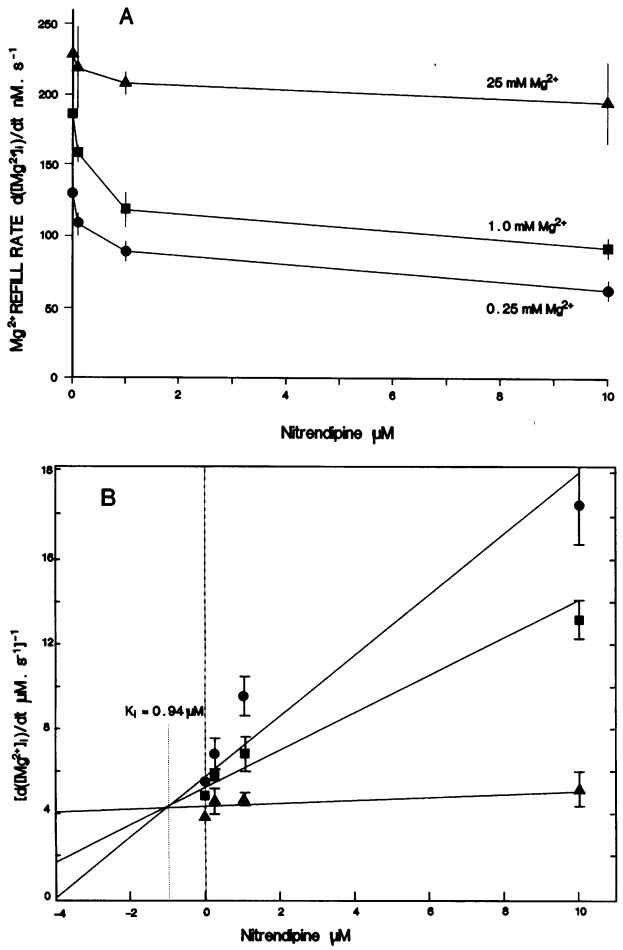

Figure 6. Effect of nitrendipine on Mg^{2+} refill in magnesium-depleted cTAL cells. (*A*) The rate of Mg^{2+} refill, $d([Mg^{2+}]_i)/dt$, was determined with the given nitrendipine concentrations using methods similar to those in Fig. 5 but with external magnesium concentrations of 0.25, 1.0, and 25 mM. (*B*) The apparent K_i value was determined as the mean of the intercepts of the three regression lines representing $d([Mg^{2+}]_i)/dt$ at the various inhibitor concentrations. Values are means±SE.

inhibitors were added to the culture media 20 min before placing the cells in magnesium-free media and during the 4-h adaptive phase. Basal Mg^{2+} levels and refill rates were determined after 4 h in magnesium-free media in the presence of the inhibitor.

Actinomycin D treatment inhibited the adaptive response by 86% (Table V), but had no effect on basal $[Mg^{2+}]_i$, and refill in cells cultured in media containing normal amounts of magnesium (data not shown). In order to determine if actinomycin D may directly alter transport, cTAL cells were first adapted for 16 h in magnesium-free media and then exposed to actinomycin D for 4.5 h. Actinomycin D did not significantly alter Mg^{2+} refill in cells adapted before treatment with the protein synthesis inhibitors (Table V). Cycloheximide inhibited the adaptive response as measured by Mg^{2+} refill rate inhibited by 60% and cordycepin by 55% (Table V). Again, no effect was observed on basal $[Mg^{2+}]_i$ in cells cultured in normal cells. These results suggest that protein synthesis is partially involved with the adaptation of transport sites in cTAL cells after placement in magnesium-free media.

Table III. Effects of Na^+ Channel Antagonists on Influx Pathway

	Concentration	$d([Mg^{2+}]_i)/dt$	Inhibition	(*n*)
	μM	*nM·s⁻¹*	*Percentage of control*	
Control		186±10	100±5	(4)
Quinidine	100	160±63	86±34	(2)
Tetrodotoxin	10	177±17	95±9	(3)
Amiloride	1000	186±23	100±12	(3)
Dichlorobenzamil	100	135±6	73±3*	(3)

Mg^{2+} influx was determined in magnesium-depleted cells as illustrated in Fig. 3 except the external magnesium concentration was 1.0 mM in the refill solution. Values are mean±SE. * Significance ($P < 0.05$) from control values.

Discussion

The thick ascending limb of Henle's loop reabsorbs 50–60% of the magnesium filtered through the glomerulus (3). The epithelial cells of the thick ascending limb also provide the sensitive controls for magnesium balance (1). Recently, de Rouffignac and colleagues have shown that the cortical segment appears to be directly involved with magnesium absorption as little, if any, magnesium transport was observed in the medullary segment (1, 5). The early microperfusion work of Shareghi and Agus using rabbit cTAL segments demonstrated that much of the absorption is passive in nature, likely through the paracellular pathway (4). More recent studies by de Rouffignac and colleagues reported that magnesium absorption may be markedly stimulated in cTAL segments by glucagon and antidiuretic hormone (2, 5). Both hormones increased magnesium with little change in transepithelial potential or resistance and no alteration in NaCl absorption suggesting that a portion of the absorption may be active in nature. Active transport would

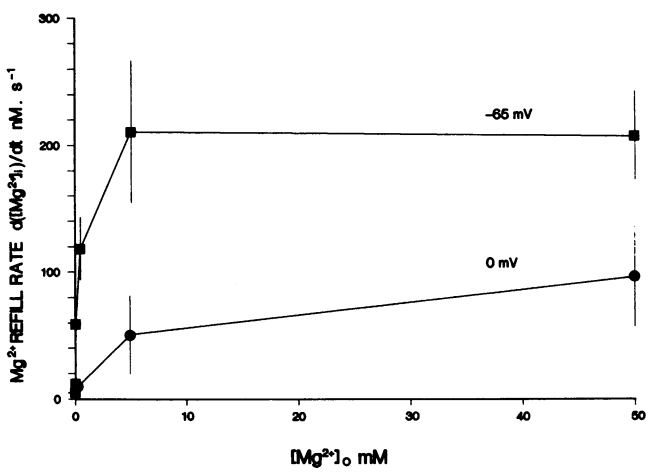

Figure 7. Concentration-dependence of Mg^{2+} refill in magnesium-depleted cTAL cells. Cells were cultured in nominally magnesium-free media for 16 h. The refill rate of $[Mg^{2+}]_i$, $d([Mg^{2+}]_i)/dt$, was assessed at the external magnesium concentrations indicated. Refill was assessed in normal magnesium-depleted cells with an apparent transmembrane voltage of −65 mV with respect to outside, and in cells treated with 100 μM ouabain and 2 μM gramicidin D to abolish the potential (see text for methods). Values are means±SD.

Table IV. Effect of Voltage on Mg^{2+} Refill Rate in Magnesium-depleted cTAL Cells

	Refill with 0.25 mM			Refill with 5 mM			Refill with 50 mM		
	$[Mg^{2+}]_i$	$d([Mg^{2+}]_i)/dt$	(n)	$[Mg^{2+}]_i$	$d([Mg^{2+}]_i)/dt$	(n)	$[Mg^{2+}]_i$	$d([Mg^{2+}]_i)/dt$	(n)
	mM	*nM·s⁻¹*		*mM*	*nM·s⁻¹*		*mM*	*mM·s⁻¹*	
Control	0.24	97		0.27±0.07	210±56	(6)	0.25±0.01	208±34	(4)
Ouabain + gramicidin	0.24±0.02	5±26	(5)	0.25±0.04	46±32	(5)	0.26±0.07	92±39	(5)
Depolarization solution	0.28±0.05	−2±30	(5)	0.27±0.08	18±28	(5)	0.26±0.06	7±24	(5)

In order to abolish the transmembrane electrical potential, cTAL cell monolayers were treated with ouabain 100 μM and gramicidin 2 μM or depolarization solution containing (in mM) KCl 118, NaCl 25, $CaCl_2$ 1, KH_2PO_4 1, glucose 18, and Hepes-Tris, 14 mM, pH 7.4. $d([Mg^{2+}]_i)/dt$ was assessed as given in Fig. 1.

necessitate transcellular magnesium movement. The present studies demonstrate that Mg^{2+} uptake into cTAL cells is greater after magnesium depletion. Although these studies do not assess transepithelial magnesium transport, they may bear on the transcellular uptake of magnesium and thus the active portion of the absorptive process. Alternatively, these processes may only be of a house-keeping nature, maintaining intracellular Mg^{2+} at optimum levels necessary for cell metabolism. Further studies are required to quantitate transcellular and paracellular movements.

Cytosolic free Mg^{2+} concentration of cTAL cells is in the order of 0.5 mM. This is ~ 1–2% of the total magnesium, the remainder being complexed to various organic and inorganic ligands and chelated within the mitochondria (6, 35–42). Presumably, it is the free Mg^{2+} which enters into biochemical processes and crosses plasma membranes. The present data indicates that Mg^{2+} enters the cell down an electrical gradient through specific pathways which are highly regulated, in part, by intracellular $[Mg^{2+}]_i$. Influx of Mg^{2+} is concentration dependent and altered by the transmembrane voltage (present data). The efflux pathway remains to be described. This is presumably active or secondary active because the normal transmembrane electrical potential is about −65 mV, inside with respect to outside (43).

We used magnesium-depleted cells to demonstrate Mg^{2+} entry because the fluorescent dye is not sufficiently sensitive to detect changes in $[Mg^{2+}]_i$ in normal cells. Mg^{2+} entry pathways, as assessed by the Mg^{2+} refill rate (15), is inhibited by a number of inorganic cations but not Ca^{2+} or Sr^{2+}. The approximate potency sequence was: $Mn^{2+} \simeq La^{3+} \simeq Gd^{3+} \simeq Ni^{2+} \simeq Zn^{2+} \simeq Be^{2+} \gg Ba^{2+} \simeq Co^{2+} \simeq Cd^{2+} \simeq Sr^{2+} \simeq Ca^{2+}$. Moreover, net ^{28}Mg uptake but not ^{45}Ca, is enhanced by magnesium depletion. Finally, $[Ca^{2+}]_i$ is not altered by magnesium depletion nor by the process of Mg^{2+} refill. Accordingly, the Mg^{2+} influx pathway appears to be separate from Ca^{2+} channels in these epithelial cells.

The Mg^{2+} entry into cTAL cells is different from similar entry pathways demonstrated in chick embryonic cardiac cells (12). These studies, performed under similar conditions as given here, showed an inhibitory potency sequence of inorganic cations of: $Ca^{2+} \simeq Sr^{2+} \simeq Ni^{2+} \simeq Co^{2+} \simeq Ba^{2+} \gg Zn^{2+} \simeq Cd^{2+} \simeq Mn^{2+}$ (12). This sequence in cardiac embryonic ventricular cells is quite different from that observed here in cTAL epithelial cells. This would suggest that there are a number of Mg^{2+} pathways which may be specific to different cell types. The notion of a population of different Mg^{2+} pathways which are organ specific is not surprising, as this has also been demonstrated for Ca^{2+} channels (17–19, 44). It should also be noted that Mg^{2+} does not share the Ca^{2+} channel in cardiac or vascular smooth muscle cells (reviewed in reference 44). Although large amounts of Mg^{2+} inhibit Ca^{2+} movement through the L-type Ca^{2+} channel, Mg^{2+} is not measurably permanent (44). This is supported by the observation that Ba^{2+}, which readily crosses the Ca^{2+} channel (17–19) does not enter through the Mg^{2+} channel (deduced from data given here).

The organic channel blockers, nifedipine, verapamil, and diltiazem, inhibit Mg^{2+} entry into magnesium-depleted cTAL cells. These drugs appear to act at different sites along the length of the variously described Ca^{2+} channels particularly the L-type channels (17–19). It would appear that these sites are also common to the Mg^{2+} pathways. Bay K 8644, an agonist of Ca^{2+} channels, also increases Mg^{2+} entry into cTAL cells. Further studies are required to determine if analogues of these or other agents may alter Mg^{2+} entry without affecting Ca^{2+} channels.

The Mg^{2+} entry pathway described here may be a channel which has a close homology to the well known Ca^{2+} channels but differ somewhat in selectivity. This notion is based on the observation that the Ca^{2+} channel blockers (nifedipine, verapamil, and diltiazem) inhibit Mg^{2+} uptake. Sodium does not

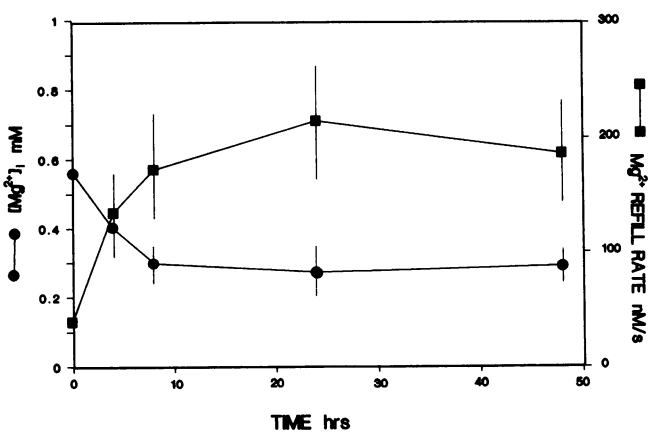

Figure 8. Time-course of magnesium-depletion in cTAL cells. Cells were placed in low magnesium media and basal $[Mg^{2+}]_i$ was measured at various times indicated. Refill was assessed by techniques given in Fig. 1. Intracellular $[Ca^{2+}]$ was not altered by magnesium-depletion or during the refill maneuver (data not shown). Values are means±SD.

Table V. Effect of Protein Synthesis Inhibitors on the Adaptive Increase in Mg^{2+} Influx

	Inhibitor present during adaptation			Inhibitor present after adaptation		
	$[Mg^{2+}]_i$	$d([Mg^{2+}]_i)/dt$	Inhibition	$[Mg^{2+}]_i$	$d([Mg^{2+}]_i)/dt$	Inhibition
	mM	$nM \cdot s^{-1}$	*percentage of control*	*mM*	$nM \cdot s^{-1}$	*percentage of control*
Control	0.40±0.04	134±41	100	0.26±0.02	213±70	100
(*n*)		(4)			(5)	
Actinomycin D	0.29±0.03	19±34	14±6*	0.25±0.04	176±27	83±15
(*n*)		(4)			(5)	
Cordycepin	0.38±0.05	54±16*	40±12*	0.26±0.07	148±17	69±8*
(*n*)		(4)			(3)	
Cyclohexamide	0.32±0.09	61±28*	45±21*	0.26±0.01	163±46	77±22
(*n*)		(5)			(5)	

Effect of protein synthesis inhibitors on adaptation of cTAL cells to low magnesium media. With the inhibitors present during adaptation, the cTAL monolayers were treated with actinomycin D (5 μg/ml), cycloheximide (50 μM), or cordycepin (100 μM) for 20 min before and after placement of the cells into magnesium-free media for 4 h. In the studies in which the inhibitor was present after adaptation, cTAL cells were adapted for 16 h before treatment with the respective protein synthesis inhibitors, the inhibitors were present for 4.5 h before $d([Mg^{2+}]_i)/dt$ was determined. Basal $[Mg^{2+}]_i$ and the refill rate was monitored by methods given in Fig. 1. * Significance ($P < 0.05$) from respective control values.

appear to be involved with Mg^{2+} refill as a number of agents and maneuvers were without effect (Table III). These speculations are not without precedent as recent electrophysiological studies have provided evidence for Mg^{2+} channels (45–47). Further experiments of a similar nature are needed to define the Mg^{2+} refill process reported here.

Extracellular magnesium concentration is normally in the order of 0.5 mM, which is similar to cytosolic Mg^{2+} levels. Accordingly, transmembrane concentration gradients are not sufficient for Mg^{2+} entry. A possible driving force for movement of Mg^{2+} across the membrane into the cell is the transmembrane electrical potential amounting to some −65 mV inside with respect to outside (43). Studies reported here support this notion. Abolishing the transmembrane voltage either through the use of ouabain and Na^+ ionophores or with K^+ solutions decrease Mg^{2+} entry; however, the entry may be sustained by enhancing the transmembrane magnesium concentration gradient (Fig. 7). Assuming divalent ion movement, an equilibrium concentration gradient of ~ 100-fold; i.e., 0.05 mM outside to 0.5 mM inside, would normally be expected based on the Nernst equation (43). However, the cells maintain $[Mg^{2+}]_i$ even when cultured for prolonged periods of time in high Mg media (present data). This is presumably due to regulation of entry and exit pathways. On the other hand, cells with this transmembrane voltage should maintain their basal Mg^{2+} levels until the outside free Mg^{2+} concentration diminishes to 0.05 mM or ~ 0.1–0.2 mM total magnesium provided that Mg^{2+} entry is entirely dependent on the voltage.

The present data indicates that Mg^{2+} entry rate into cTAL cells is dependent on the external concentration. Fig. 7 shows the association of $d([Mg^{2+}]_i)/dt$ with external magnesium concentrations in normal cells. The concentration-dependence of Mg^{2+} entry is saturable and can be described by Michaelis-Menten kinetics with an apparent J_{max} of 210±18 $nM \cdot s^{-1}$ and K_m of 0.27±0.12 mM. The kinetics parameters are altered by the transmembrane voltage as the saturation rate and apparent affinity decreased when the transmembrane voltage was abolished (22).

The response of cTAL cells to magnesium-free culture media is relatively rapid; detectable within 1–2 h. It is interesting, however, that the increase in Mg^{2+} refill rate is not maximal until ~ 4–6 h. This may suggest that in addition to increasing the entry rate there may also be recruitment of new or formed transporters into the apical membrane. To test this possibility we used a number of agents known to inhibit protein synthesis and translation steps. Cycloheximide, through its rapid action to block protein elongation, has been widely used to inhibit protein synthesis. Inhibition of the de novo protein synthesis by the use of cycloheximide resulted in diminution of the adaptive response, as assessed by the Mg^{2+} refill rate, by ~ 50%. Accordingly, part of the enhanced Mg^{2+} uptake is dependent on de novo protein synthesis. The onset of the cellular effects of protein synthesis inhibition are directly related to the rapidity of the turnover of a specific protein. Cycloheximide resulted in rapid inhibition of the adaptive response; accordingly, the transporters may be rapidly turning over.

To investigate the involvement of pretranslational steps in control of Mg^{2+} transport, the inhibitors, actinomycin D and cordycepin, were used before adaptation. These agents resulted in 86% and 55% decrease in the adaptive response. Thus, total mRNA synthesis (29), RNA polymerase (30), nuclear post-transcriptional polyadenylation (31–34), and perhaps other steps (31), are involved in up-regulating Mg^{2+} transport activity. The present evidence would imply that both transcriptional and post-transcriptional processes are required in adding new transport units to the membrane. Further studies will be necessary to characterize the turnover of the components known to be important in up-regulation of Mg^{2+} transport.

In summary, the present studies describe some aspects of intracellular Mg^{2+} control. These studies show that Mg^{2+} uptake into magnesium-depleted cTAL cells is rapid and facilitated. These studies also suggest that Mg^{2+} entry into isolated cTAL cells possess some specificity for Mg^{2+} and is regulated, in part, by $[Mg^{2+}]_i$. How relevant these studies are to transepithelial magnesium reabsorption in the thick ascending limb remains to be determined.

Acknowledgments

We gratefully acknowledge the excellent secretarial assistance of H. Hall in the preparation of the manuscript.

This work was supported by research grants from the Medical Research Council of Canada (MT-5793) and the Kidney Foundation of Canada.

References

1. DeRouffignac, C., J. M. Elalouf, and N. Rionel. 1987. Physiological control of the urinary concentrating mechanism by peptide hormones. *Kidney Int.* 31:611–620.

2. Quamme, G. A. 1989. Control of magnesium transport in the thick ascending limb. *Am. J. Physiol.* 256:F197–F210.

3. Morel, F., N. Roinel, and C. Le Grimellec. 1969. Electron probe analysis of tubular fluid composition. *Nephron.* 6:350–364.

4. Shareghi, G. R., and Z. S. Agus. 1982. Magnesium transport in the cortical thick ascending limb of Henle's loop of the rabbit. *J. Clin. Invest.* 69:759–769.

5. Wittner, M., A. Di Stefano, P. Wangemann, R. Nischke, R. Greger, C. Bailly, C. Amiel, N. Roinel, and C. De Rouffignac. 1988. Differential effects of ADH on sodium, chloride, potassium, calcium and magnesium transport in cortical and medullary thick ascending limbs of mouse nephron. *Pflügers Arch.* 412:516–523.

6. Flatman, R. W. 1984. Magnesium transport across cell membranes. *J. Memb. Biol.* 80:1–44.

7. Raju, B., E. Murphy, L. A. Levy, R. D. Hall, and R. E. London. 1989. A fluorescent indicator for measuring cytosolic free magnesium. *Am. J. Physiol.* 256:C540–C548.

8. Smith, W. L., and A. Garcia-Perez. 1985. Immunodissection: use of monoclonal antibodies to isolate specific types of renal cells. *Am. J. Physiol.* 248:F1–F77.

9. Allen, M. L., A. Nakao, W. K. Sonnenburg, M. Burnatowska-Hledin, W. S. Spielman, and W. L. Smith. 1988. Immunodissection of cortical and medullary thick ascending limb cells from rabbit kidney. *Am. J. Physiol.* 255:F704–F710.

10. Nakao, A., M. L. Allen, W. K. Sonnenburg, and W. L. Smith. 1989. Regulation of cAMP metabolism by PGE2 in cortical and medullary thick ascending limb of Henle's loop. *Am. J. Physiol.* 256:C652–C657.

11. Kim, H. D., Y.-S. Tsai, C. C. Franklin, and J. T. Turner. 1988. Characterization of $Na^+/K^+/Cl^-$ cotransport in cultured HT29 human colonic adenocarcinoma cells. *Biochim. Biophys. Acta.* 946:397–404.

12. Quamme, G. A., and S. W. Rabkin. 1990. Cytosolic free magnesium in cardiac myocytes: characterization of magnesium influx pathway. *Biochem. Biophys. Res. Commun.* 167:1406–1412.

13. Grynkiewicz, G., M. Poenie, and R. Y. Tsien. 1985. A new generation of Ca^{2+} indicators with greatly improved fluorescence properties. *J. Biol. Chem.* 260:3440–3450.

14. Elin, R. J., and E. Johnson. 1982. A method for the determination of magnesium content of blood mononuclear cells. *Magnesium.* 1:115–121.

15. Quamme, G. A., and L-J. Dai. 1990. Presence of a novel influx pathway for Mg^{2+} in MDCK cells. *Am. J. Physiol.* 259:C521–C525.

16. Shafik, I. M., and G. A. Quamme. 1989. Early adaptation of renal magnesium reabsorption in response to magnesium restriction. *Am. J. Physiol.* 257:F974–F977.

17. Glossmann, H., and J. Striessnig. 1990. Molecular properties of calcium channels. *Rev. Physiol. Biochem. Pharmacol.* 114:1–105.

18. Porzig, H. 1990. Pharmacological modulation of voltage-dependent calcium channels in intact cells. *Rev. Physiol. Biochem. Pharmacol.* 116:210–262.

19. Pelzer, D., S. Pelzer, and T. F. McDonald. 1990. Properties and regulation of calcium channels in muscle cells. *Rev. Physiol. Biochem. Pharmacol.* 114:108–148.

20. Enyeart, J. J., B. A. Biagi, R. N. Day, S.-S. Sheu, and R. A. Maurer. 1990. Blockade of low and high threshold Ca^{2+} channels by diphenylbutylpiperidine antipsychotics linked to inhibition of prolactin gene expression. *J. Biol. Chem.* 265:16373–16379.

21. Féray, J.-C., and R. Garay. 1987. A one-to-one Mg^{2+}:Mn^{2+} exchange in rat erythrocytes. *J. Biol. Chem.* 262:5763–5768.

22. Frenkel, E. J., M. Graziani, and H. J. Schatzmann. 1989. ATP requirement of the sodium-dependent magnesium extrusion from human red blood cells. *J. Physiol. (Lond.).* 414:385–397.

23. Günther, T., J. Vormann, and V. Höllriegl. 1990. Characterization of Na^+-dependent Mg^{2+} efflux from Mg^{2+} loaded rat erythrocytes. *Biochim. Biophys. Acta.* 1023:455–461.

24. Gonzalez-Serratos, H., and H. Rasgado-Flores. 1990. Extracellular magnesium-dependent sodium influx in squid giant axons. *Am. J. Physiol.* 259:C541–C548.

25. Simchowitz, L., M. A. Foy, and E. J. Cragoe, Jr. 1990. A role for Na^+/Ca^{2+} exchange in the generation of superoxide radicals by human neutrophils. *J. Biol. Chem.* 265:13449–13456.

26. Kaczorowski, G. J., R. S. Slaughter, V. F. King, and M. L. Garcia. 1989. Inhibition of sodium-calcium exchange: Identification and development of probes of transport activity. *Biochim. Biophys. Acta.* 988:287–302.

27. Hess, P., J. B. Lansman, and R. W. Tsien. 1986. Calcium channel selectivity for divalent and monovalent cations: voltage and concentration dependence of single channel current in ventricular heart cells. *J. Gen. Physiol.* 88:293–319.

28. Pope, A. J., I. R. Jennings, D. Sanders, and R. A. Leigh. 1990. Characterization of Cl^- transport in vascular membrane vesicles using a Cl^--sensitive fluorescent probe: reaction kinetic models for voltage and concentration-dependence Cl^--flux. *J. Membr. Biol.* 116:129–137.

29. Cooper, H. C., and R. Braverman. 1977. The mechanism by which actinomycin D inhibits protein synthesis in animal cells. *Nature (Lond.).* 269:527–529.

30. Darnel, J. E., L. Phillipson, R. Wall, and H. Adesnik. 1971. Polyadenylic acid sequences: role in conversion of nuclear RNA into messenger RNA. *Science (Wash. DC).* 174:507–510.

31. Grollman, A. P., and M. T. Huang. 1976. *In* Protein Synthesis. E. H. McConkey, editor. Marcel Decker, Inc., New York. 125–167.

32. Jelinek, W., M. Adesnik, M. Salditt, D. Sheiness, R. Wall, G. Malloy, L. Phillipson, and J. E. Darnell. 1973. Further evidence on the nuclear origin and transfer to the cytoplasm of polyadenylic acid sequences in mammalian cell RNA. *J. Mol. Biol.* 75:515–521.

33. Rossow, P., M. S. Rachos, and H. Amos. 1975. Metabolic effects of glucose starvation in animal cell cultures. *Arch. Biochem. Biophys.* 768:520–524.

34. Siev, M., R. Weinberg, and S. Penman. 1969. The selective interruption of nucleolar RNA synthesis in HeLa cells by cordycepin. *J. Cell. Biol.* 41:510–520.

35. Fry, C. H. 1986. Measurements and control of intracellular magnesium ion concentration in guinea pig and ferret ventricular myocardium. *Magnesium.* 5:306–311.

36. Blatter, L. A., and J. A. S. McGuigan. 1986. Free intracellular magnesium concentration in ferret ventricular muscle measured with ion selective microelectrode. *J. Exp. Physiol.* 71:451–465.

37. Brinley, F. J., Jr., A. Scarpa, and T. Tiffert. 1977. The concentration of ionized magnesium in barnacle muscle fibres. *J. Physiol. (Lond.).* 266:545–565.

38. Geisbuhler, T., R. A. Altschuld, R. W. Trewyn, A. Z. Ansei, K. G. Lamka, and G. P. Brierley. 1984. Adenine nucleotide metabolism and compartmentalization in isolated adult rat heart cells. *Circ. Res.* 54:536–546.

39. Murphy, E., C. Steenberger, L. A. Levy, B. Raju, and R. E. London. 1989. Cytosolic free magnesium levels in ischemic rat heart. *J. Biol. Chem.* 264:5622–5627.

40. Cohen, S. M., and C. T. Burt. 1977. ^{31}P nuclear magnetic relaxation studies of phosphocreatinine in intact muscle: determination of intracellular free magnesium. *Proc. Natl. Acad. Sci. USA.* 74:4271–4275.

41. Gupta, R. K., and R. D. Moore. 1980. ^{31}P NMR studies of intracellular free Mg^{2+} in intact frog skeletal muscles. *J. Biol. Chem.* 255:3987–3992.

42. Hess, P., and R. Weingart. 1981. Intracellular magnesium concentration determination with ion-selective microelectrodes. *J. Physiol. (Lond.).* 318:14. (Abstr.)

43. Greger, R. 1985. Ion transport mechanisms in thick ascending limb of Henle's loop of mammalian nephron. *Physiol. Rev.* 65:760–797.

44. Lansman, J. B., P. Hess, and R. W. Tsien. 1986. Blockade of current through single calcium channels by Cd^{2+}, Mg^{2+}, and Ca^{2+}: voltage and concentration dependence of calcium entry into the pore. *J. Gen. Physiol.* 88:321–347.

45. Preston, R. P. 1991. A magnesium current in Paramecium. *Science (Wash. DC).* 250:285–288.

46. Narita, K., F. Kawasaki, and H. Kita. 1990. Mn and Mg influxes through Ca channels of motor nerve terminals are prevented by verapamil in frogs. *Brain Res.* 510:289–295.

47. Nakatani, K., and K.-W. Yau. 1988. Calcium and magnesium fluxes across the plasma membrane of the toad rod outer segment. *J. Physiol. (Lond.).* 395:695–729.